Utilization of Hyper-Dendritic Zinc during High Rate Discharge in Alkaline Electrolytes

Utilization of Hyper-Dendritic Zinc during High Rate Discharge in Alkaline Electrolytes

Greg Davies,[a,b] Andrew G. Hsieh,[a,b] Marcus Hultmark,[a] Michael E. Mueller,[a] and Daniel A. Steingart[a,b,z]

[a]*Department of Mechanical and Aerospace Engineering, Princeton University, Princeton, New Jersey 08544, USA*
[b]*Andlinger Center for Energy and the Environment, Princeton University, Princeton, New Jersey 08544, USA*

Zinc is a low cost and abundant material, and its strong reducing potential combined with stability in aqueous solutions give it high energy density and safety. It is, therefore, known to be an excellent choice of anode for a wide range of battery designs. However, this material presents some challenges for use in a secondary battery, including morphology changes and dendrite growth during charge (Zn deposition), and low utilization during discharge (Zn dissolution). Low utilization is related to a combination of corrosion and passivation effects. In this paper, we demonstrate a hyper-dendritic (HD) zinc morphology that has a high surface area and allows for rapid discharge in a completely freestanding system with no binders or conductive additives, while still maintaining significantly higher utilization than typical zinc morphologies. At rates of 2.5 A/g, the HD zinc has a utilization level approximately 50% higher than typical zinc granules or dust. Furthermore, we demonstrate that, through tuning of the electrolyte with specific additives, we are able to further increase the utilization of the material at high rate discharge by up to 30%.
 [DOI: 10.1149/2.0891607jes]

Manuscript submitted September 10, 2015; revised manuscript received April 11, 2016. Published April 26, 2016.

Zinc possesses many characteristics that are favorable for large scale energy storage: high volumetric energy density, low cost, low toxicity, global abundance, and chemical compatibility with aqueous electrolytes.[1] As an example of a zinc battery application, silver-zinc batteries have been successfully used as primary and secondary cells in a range of demanding applications, including those requiring large scale, high power and high energy density. These include critical military and space applications.

However, zinc electrodes present some significant challenges, and anode failure is a key factor in the reduced cycle life of these batteries.[2] These challenges include morphology changes and dendrite growth during deposition,[3] which can lead to problems such as the short circuit of a cell, and poor utilization efficiencies during dissolution, arising mainly from corrosion and passivation effects.[1] As such, typical zinc utilization levels are limited to 60% or less.[4,5] Careful engineering and materials science can extend the cycle life of the electrode; however, the issues of morphology change and poor utilization still present major limitations for secondary batteries with a zinc electrode.[2,6]

A range of battery designs have been proposed to address some of the morphology-related problems: flow-based designs, fuel cell-like designs, and novel electrode architectures.

In flow-based systems, redox flow batteries based on chemistries such as ZnBr and ZnFe attempt to mitigate changes in electrode morphology during cycling by continuously reforming the cathode and anode. However, these systems can suffer from low energy density[7] due to the limited solubility of the dissolved redox species. Other battery designs proposed include semi-solid and flow-assisted designs where the active material is refreshed periodically.[8] These flow based approaches suffer from a significant energy overhead in the form of pumping costs to maintain the desired flow levels.

Regenerative metal/air fuel cells seek to remove the need to recharge the zinc in-situ, thereby eliminating morphology changes during cycling. This is achieved by discharging the zinc in one location and regenerating it in another. Several designs have been developed,[9,10] although as yet no large scale installations are in place. Alternatively, Zn can be plated onto substrates which avoid dendrite growth, such as cadmium, which increases deposition and dissolution efficiencies due to the high overpotential for hydrogen generation on Cd.[11] However, cadmium presents some environmental and health concerns which limit its potential adoption.

Recently, several three-dimensional zinc foam structures have been suggested to provide cyclable zinc electrodes without the problems associated with dendrite growth and morphology changes.[5,12] In addition to providing high utilization under primary discharge, these electrode structures also allow for significant improvements in cyclability, albeit at the loss of volumetric energy density. Co-deposition of nano-zinc/graphene composites have also been demonstrated, with potentially useful applications in energy storage. However, these have limited discharge efficiency in aqueous electrolytes due to rapid oxidation of the metal.[13]

In addition to the morphology-related issues during Zn plating, minimizing passivation and corrosion effects during Zn dissolution has also been a major challenge. To get a better sense of the specific issues that need to be addressed, we provide a brief overview of the Zn dissolution process. During the anodic dissolution of Zn in alkaline electrolytes, metallic zinc, Zn(s), oxidizes to aqueous Zn^{2+} ions, which form a stable complex with OH^- known as zincate, $Zn(OH)_4^{2-}$ 1. Zincate will precipitate as ZnO when the solution is saturated 2, however its solubility increases with pH,[1] which delays passivation. During discharge, if the zincate concentration exceeds the local solubility limit, ZnO will precipitate on the surface of the zinc as what is typically known as type I ZnO. This layer is loose and porous, and does not directly passivate or block the surface of the zinc.[14] However, it does impact ion transport between the electrolyte and zinc surface, impeding OH^- and zincate transport.

$$Zn\,(s) + 4OH^- \rightarrow [Zn(OH)_4]^{2-}\,(aq) + 2e^- \quad [1]$$

$$[Zn(OH)_4]^{2-}\,(aq) \rightarrow ZnO\,(s) + H_2O + 2OH^- \quad [2]$$

At high anodic overpotentials, in a zincate-saturated solution (or local environment), there is a solid state transition directly from Zn(s) to ZnO(s), without the dissolution step 3. The surface oxide film that forms is known as type II ZnO.[15] Passivation occurs when type II ZnO forms on the Zn surface, hindering any further dissolution, and any remaining zinc is effectively rendered electrochemically inactive. Therefore, any zinc trapped under the passivation layer will be not be utilized at a useful potential.

$$Zn\,(s) + 2OH^- \rightarrow ZnO\,(s) + H_2O\ + 2e^- \quad [3]$$

Based on this understanding, the ability for zincate ions to diffuse away from the Zn surface will impact the rate of ZnO growth and passivation during Zn dissolution. Therefore, passivation effects are expected to be

[z]E-mail: steingart@princeton.edu

felt more rapidly at higher current densities (i.e., high current per unit surface area).[14,16] It follows, then, that high surface area electrodes are beneficial for minimizing passivation and maximizing power output.

Unfortunately, high surface area zinc electrodes are more susceptible to corrosion through parasitic surface reactions, resulting in lower coulombic efficiencies as no charge is transferred to the external circuit. This can occur via two pathways: the first is a reaction with dissolved oxygen in the electrolyte 4, although oxygen solubility is low in concentrated salt solutions,[1] so this reaction will be limited:

$$2Zn\,(s) + O_2\,(aq) \rightarrow 2ZnO\,(s) \quad [4]$$

The second, more common corrosion pathway is a reaction between Zn and water, which results in a hydrogen evolution reaction. The hydrogen evolution half-reaction, 5, couples with the Zn oxidation half-reaction 3 to give the parasitic hydrogen evolution reaction 6:

$$H_2O + e^- \rightarrow OH^- + \frac{1}{2}H_2\,(g) \quad [5]$$

$$Zn\,(s) + H_2O\,(l) \rightarrow ZnO\,(s) + H_2\,(g) \quad [6]$$

This is a slower reaction than 4,[1] however it is highly dependent on the nature and quantity of contaminants in the system.

Both corrosion reactions are parasitic, as they consume active material without contributing any useful work (i.e., no charge flows into an external circuit). This reduces the amount of active material available to provide useful energy, and results in a decrease in utilization efficiency. Additionally, as corrosion takes place at the Zn surface, higher surface area particles are more susceptible. The use of low surface area particles can limit the effect of corrosion, but does so at the expense of more rapid passivation.[4]

To avoid the detrimental effects of corrosion and passivation, conventional zinc electrodes typically use low surface area particles in composite, powder, or paste form. Furthermore, these electrodes are typically limited to low discharge rates, known as "near-equilibrium" conditions, in which electrochemical overpotentials are minimized.

In this paper, we demonstrate that we can significantly improve the utilization efficiency of Zn dissolution at high rates, with the use of high surface-area, hyper-dendritic (HD) zinc particles,[12] and illustrate their advantage versus standard, lower surface area zinc granules and dust.

Another approach to optimizing the performance of Zn electrodes is the incorporation of a range of additives. As an example, these include ZnO to reduce corrosion,[1] LiOH to hinder formation of a dense passivating layer,[17] and bismuth to reduce dendrite growth.[18]

In addition to the use of HD Zn particles, this paper also investigates the use of additives to enhance the high-rate utilization of zinc. The additives were selected based on their ability to delay passivation (thus increasing utilization) either by increasing the solubility of zincate or by modifying the ZnO layer:

- *Potassium Citrate:* citrate is a known chelating which complexes with zincate, improving zincate solubility. The ions are believed to form a zincate-citrate compound with a polymeric structure, which stabilizes the zincate in solution. This correspondingly increases zincate solubility,[19] which we hypothesize has the effect of delaying ZnO formation.
- *Potassium Chloride*: It is proposed in literature that chloride ions may react with zincate to form a zinc hydroxychloride complex that has a higher solubility than zincate,[20] thus it is our hypothesis that it will hinder the formation of ZnO and increase utilization.
- *Sodium dodecylbenzenesulfonate (SDBS)*: SDBS is an anionic surfactant. During zinc discharge, SDBS adsorbs onto the metal surface, altering the morphology of ZnO passivating layers by making them more porous and less dense.[21] This leads to the formation of a surface layer that leaves the zinc accessible despite ZnO formation.

This study focuses on the limits of utilization and the high rate performance of several zinc morphologies. Diffusion and other porous electrode effects are minimized by studying small active masses in the absence of binders and conductive additives. The utilization, or utilization efficiency, of a material is defined as the amount of charge that can be usefully extracted within a given voltage window, divided by the theoretical specific capacity of the material (in the case of zinc, 820 mAh/g). We show that high utilization efficiencies of greater than 75% can be achieved at high discharge rates, >3C, and a useful capacity, 45% for HD Zn compared with 0% for granules or dust, is achievable at rates up to 20C based on the mass of Zn, by optimizing particle size and morphology. We also show that the use of electrolyte additives, and optimizing the concentration of the alkaline electrolyte are beneficial for maximizing utilization. The work presented here demonstrates the benefits of using high surface area dendritic zinc and deserves consideration in cell designs which are oriented toward high-power, high-utilization operation.

Experimental

Three types of Zn particles were used in this study: Zn granules (Sigma Aldrich), Zn dust (Sigma Aldrich), and HD Zn, a nanostructured Zn particle. HD Zn is produced via electrodeposition onto Ni wire or wire mesh at high overpotentials (−2.0 V vs. Hg/HgO) from a 8.9 M KOH/0.61 M saturated ZnO solution; further details on the formation and properties of HD Zn are described elsewhere.[12] After deposition, the hyper-dendritic Zn was washed first with deionized (DI) water, then with 0.01 M H_2SO_4, and again with DI water. The resulting powder was vacuum dried and ground by hand with a mortar and pestle.

In a typical utilization experiment, ∼20 mg of dry Zn granules, dust or powdered HD Zn is spread over a ∼1 cm^2 area on a copper foil current collector placed in a rectangular cell; this constitutes the working electrode (WE). The Zn was freestanding with no additives or binders used. Nickel mesh was used as the counter electrode within the cell, with a small strip of Zn plate used as the reference electrode. Once ready for testing, the desired electrolyte was then slowly added until the cell was flooded (∼6 mL). In this configuration, the small masses of zinc remain freely sitting on the current collector, within the electrolyte bath; no compression was applied, nor were any conductive fillers or binding agents used, unlike in conventional electrodes.

The utilization (i.e., the ratio of extractable capacity to theoretical capacity, discussed further below) of each particle type and electrolyte composition was measured by galvanostatically discharging the small mass of particles using mass-specific currents of ∼0.05, 0.2, 0.5, 1.0, and 2.5 A/g. Further experiments at 10 A/g and 25 A/g were conducted on the HD Zn. A representative galvanostatic discharge curve is shown in Figure 1, demonstrating how the potential of the WE changes as a function of discharge time for a typical Zn particle sample in an aqueous KOH electrolyte. Also shown is the measured discharge time (t_{meas}), which we take as the time at which the WE potential exceeds a cutoff potential of +0.6 V vs. Zn/Zn^{2+}, and the theoretical discharge time (t_{theor}), which we calculate for each sample from:

$$t_{theory} = \frac{Q_{Zn} \cdot m_{Zn}}{I} \quad [7]$$

where Q_{Zn} is the theoretical capacity of Zn (∼820 mAh/g), m_{Zn} is the mass of Zn particles being discharged, and I is the applied discharge current. We then calculate the electrochemical utilization efficiency (% utilization) for each sample from:

$$\%\ utilization = \frac{t_{\text{measured}}}{t_{theory}} \cdot 100\% \quad [8]$$

which represents the amount of useful capacity that was extracted from the Zn sample as a percentage of the theoretical capacity. To ensure that no current was measured from competing parasitic processes on the copper current collector alone, a galvanostatic discharge was measured on the current collector with the base electrolyte and no zinc. Within the cutoff range, no capacity was seen to be contributed from the copper, and therefore we can assume that the utilization can be attributed to effects on the Zn.

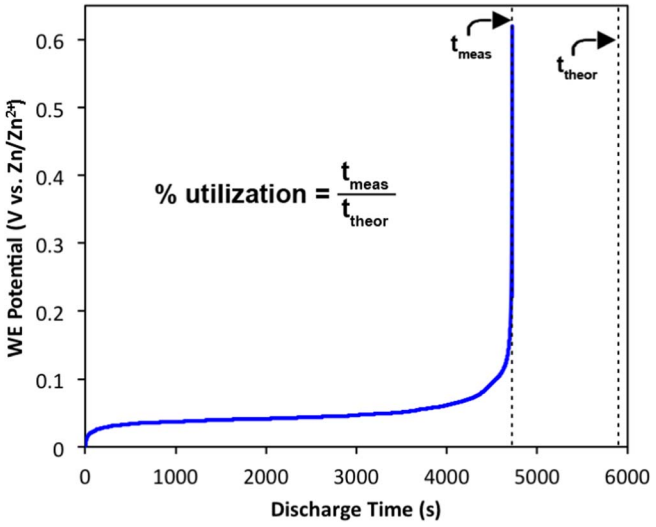

Figure 1. Representative example of the change in working electrode (WE) potential as a function of time during the galvanostatic discharge of Zn particles in aqueous KOH. Theoretical and measured discharge times t_{theor} and t_{meas}, respectively, are indicated by vertical dashed lines.

As described later, a variety of these tests were run with varying electrolyte concentrations and several additives, to determine the effect of system conditions and morphology on utilization efficiency.

Electrochemical experiments were carried out with a Gamry Reference 3000 potentiostat. Surface area measurements of the Zn particles were conducted with a Micromeritics Gemini V Series surface area analyzer, using small volume sample holders with filler rods, from nitrogen adsorption isotherms following the Brunauer, Emmett, and Teller (BET) method. Electron microscopy was conducted with a Quanta 200 FEG environmental scanning electron microscope (ESEM).

Results and Discussion

Utilization of zinc under various discharge conditions.—Figure 2 shows SEM images of the three types of Zn particles used in this study, along with their mass-specific surface areas as measured by nitrogen adsorption (BET). Zn granules are irregularly-shaped particles, with dimensions on the order of 100–500 μm and a surface area of ∼0.1 m^2/g. The morphology is these particles is similar to that used in a range of consumer primary alkaline cells. The Zn dust particles are spherical in shape, with diameters on the order of 1–10 μm and a surface area of ∼0.3 m^2/g. This morphology is similar to zinc used in pasted zinc electrodes.[22]

Hyper-dendritic Zn particles have an overall size of 10–20 μm, with sub-micron structural features.[12] All types of particles are morphologically distinct, and the surface area of HD Zn is significantly larger than the two commercial Zn particles. BET measurements were conducted on ∼0.4 g masses of HD Zn. Results showed that surface area was sensitive to synthesis method. Between different syntheses, surface areas varied from 1.9 to $3.4\frac{m^2}{g}$. Within each HD Zn batch, measurements of surface area ranged $+/-\ 0.15\frac{m^2}{g}$. Figure 3 shows SEM images of the three types of Zn particles partially discharged at a rate of 2.5 A/g, showing the surface morphology. Of particular note is the HD Zn which morphology maintains its dendritic, high-surface area nature.

Figure 4 shows the utilization efficiency as a function of discharge rate for the three zinc particle types at a fixed 4 M KOH electrolyte concentration. All types of zinc show a clear peak in utilization efficiency at mid-range currents, with utilization decreasing both toward the low and high current regions. The Zn granules and dust have similar utilization trends, with the peak utilization at a similar current and magnitude (∼80–90% at 0.2 A/g). HD Zn shows the same overall trend, however, the peak utilization efficiency of HD Zn is observed to be shifted to a higher current as compared with the other morphologies. This results in HD Zn having a much higher utilization at high rates than the other morphologies, which will be described in further detail below.

In this system, low utilization efficiencies during discharge can be related to several effects. Direct consumption of metallic zinc through corrosion mechanisms can reduce the amount of material directly available for discharge. However, isolation of active material from either ionically or electronically conducting pathways is also known to be a significant contributor to utilization loss in zinc batteries.[23–25] Loss of ionic contact can occur through the formation of passivation layers that effectively block active material from the electrolyte, isolating material that cannot be utilized. Loss of electronic contact can occur either by formation of a passivation layer at the zinc/current collector interface, or through a loss of material leading to loss of contact with the current collector. We argue that the dominating mechanism depends on the specific discharge current. We first introduce simple models explaining the key utilization trends for each of the corrosion and passivation mechanisms, and use this to help explain the system behavior and particle performance in the different current regions.

As explained previously, corrosion is a parasitic side reaction that consumes Zn without producing any useful work, and occurs concurrently and in direct competition with the desired electrochemical reaction. At lower currents, parasitic corrosion reactions are relatively more dominant (as compared with passivation), as they form a higher proportion of the total dissolution reaction. As corrosion is a surface reaction, its rate scales with the surface area of the Zn particle and is proportional to the time in the electrolyte. This behavior can be modeled by considering the total charge that is parasitically lost to corrosion during discharge, Q_{corr}:

$$Q_{corr} = A * j_{corr} * t_{disc} \quad [9]$$

where A is area over which corrosion is acting, j_{corr} is the corrosion current density, and t_{disc} is the discharge time, which is inversely proportional to the discharge rate i_{disc}. Therefore, the effect of discharge rate on Zn utilization, considering corrosion effects only, can be

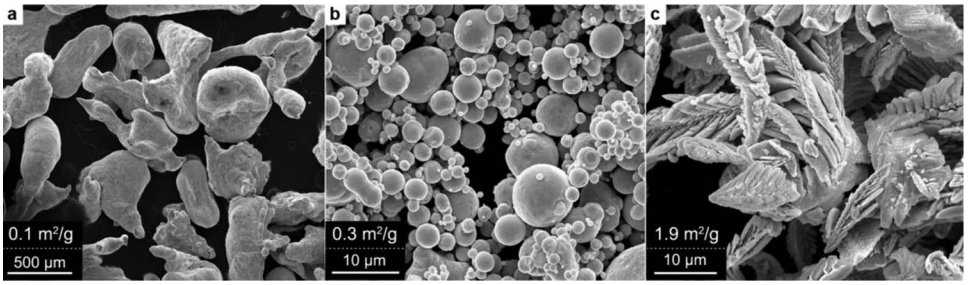

Figure 2. SEM images and mass-specific surface areas of the (a) Zn granules, (b) Zn dust, and (c) hyper-dendritic Zn particles used in this study.

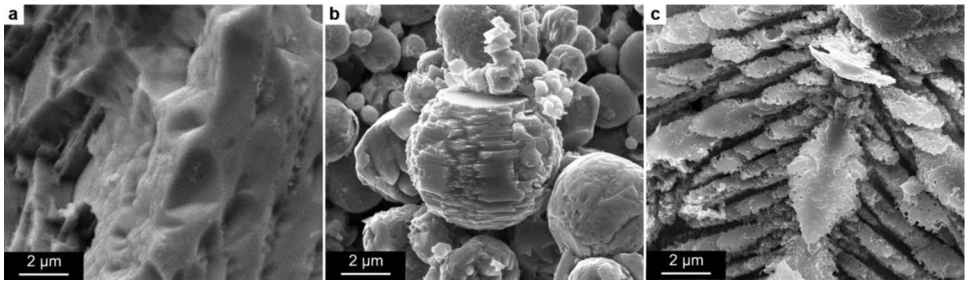

Figure 3. SEM images of (a) Zn granules, (b) Zn dust, and (c) HD Zn particles after discharge in 8.9 M KOH at a 2.5 A/g rate.

expressed as:

$$Utilization_{\text{Corr}} = 1 - \frac{A * j_{corr} * t_{disc}}{Q_{total}}$$
$$= 1 - \frac{A * j_{corr}}{i_{disc}} \quad [10]$$

Q_{total} is the theoretical total charge, which is equal to sum of the contribution from corrosion and discharge currents. Note that surface area and corrosion current vary during discharge. From 10, the change in Zn utilization efficiency due solely to corrosion effects (as a function of discharge current) is plotted in Figure 5. Although simplistic, this model shows that at lower currents, parasitic corrosion reactions are relatively more important (i.e., utilization efficiency is lower), as they form a higher proportion of the total dissolution reaction. Conversely, the corrosion term in 10 is minimized at high discharge currents, and utilization efficiency increases as Zn is electrochemically reacted faster than it can corrode. Furthermore, a high surface area material such as HD Zn will experience a higher rate of parasitic corrosion reactions and therefore performs worse than low surface area materials at low current.

A quantitative estimate of corrosion on total utilization at low currents is shown below in Table I. Using equilibrium and kinetic data[12,26] of hydrogen evolution and zinc dissolution in alkaline solution, an Evans Diagram was constructed to estimate the loss in utilization from corrosion, shown in Figure 6. The Evans Diagram estimates the reaction rates of each of the hydrogen evolution 3 and zinc dissolution 5 half-reactions over a range of potentials, assuming Tafel kinetics. The oxygen reduction mechanism 4 has been ignored given the low solubility of oxygen in high concentration salt solutions. At the system equilibrium potential, the current from each half reaction will be equal, in order for the zinc dissolution/hydrogen evolution redox couple to balance (conservation of charge). This allows for an estimate of the corrosion current on the surface of the zinc.

The hydrogen evolution reaction is clearly seen as the limiting reaction in these cases, and results in a system equilibrium potential that is equal to the equilibrium potential of the zinc dissolution reaction. Therefore, we estimate the corrosion current density to be equal to rate of hydrogen evolution at the zinc dissolution equilibrium potential, as shown in Figure 6.

As both half reactions occur on the surface of zinc, we can calculate absolute corrosion current by multiplying current density by the particle surface area. With this factored in, the HD Zn clearly shows a higher corrosion current than granular zinc, and the trend of better utilization for granular versus HD Zn at low currents is clearly displayed. However, while the trends hold, the calculated utilization efficiencies do not match the experimentally-measured values, suggesting that corrosion alone does not fully explain the utilization magnitude for both types of zinc. It is proposed that this is related to loss of contact between the zinc and current collector, as described in more detail below.

Another mechanism that limits Zn utilization is passivation, or the formation of a ZnO layer on the surface of the discharging zinc. As the passivation layer builds up, the surface of the zinc becomes blocked off from the electrolyte and unreacted zinc becomes inaccessible. Several relationships have been proposed to link passivation time to current.[16] For diffusion-dominated mechanisms, the supersaturation of zincate, the diffusion of OH^- through the porous ZnO passivation

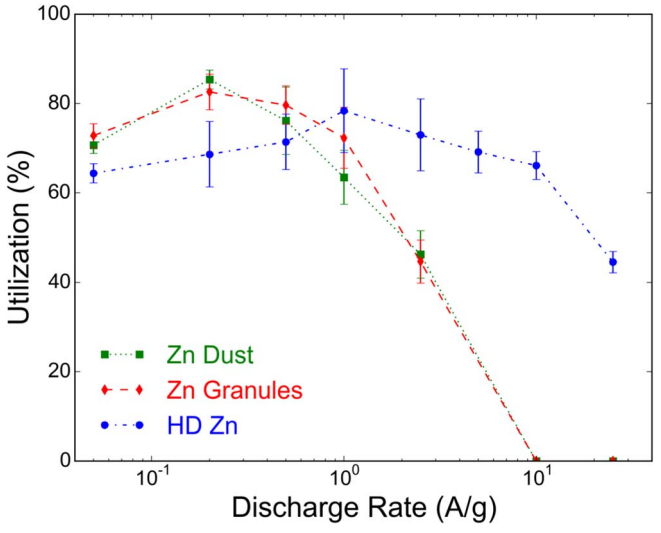

Figure 4. Comparison of the utilization efficiencies (% utilization) of Zn granules, Zn dust and dendritic Zn samples that were discharged galvanostatically in 4 M KOH at mass-specific currents of 0.05, 0.2, 0.5, 1.0, 2.5, 5, 10 & 25 A/g. Log scale x-axis.

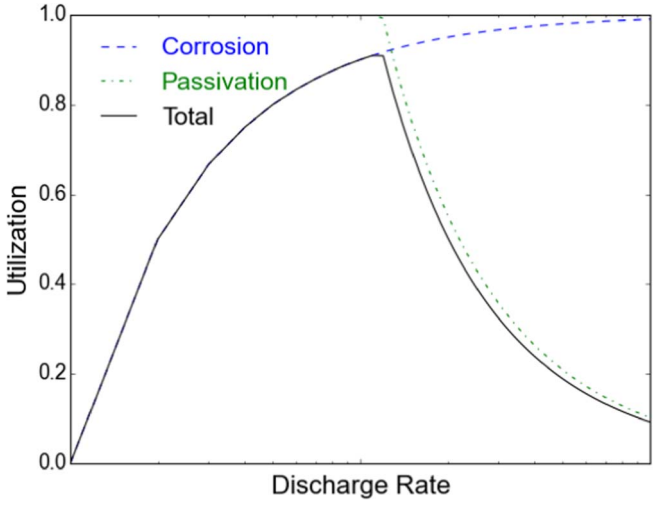

Figure 5. A simple model showing the loss in utilization due to corrosion alone 10 [blue dashed line], passivation alone 12 [red dot-dash line], and the combined corrosion and passivation [black solid line] impact on utilization. Log scale x-axis. No isolation or current collector contact effects are considered.

Table I. Calculated corrosion currents from Evans Diagram. The calculated utilization displays similar trends to those seen in the experiments, however estimates a much higher utilization across all zinc types than was seen. This difference is believed to be caused by current collector contact and material isolation effects.

Morphology	i_{corr}	Calculated utilization at 4 mA for a constant corrosion rate	Actual Utilization at 4mA
HD Zinc	0.49 mA	89%	68.7 +/− 7.3%
Zinc Dust	0.14 mA	97%	85 +/− 2%
Zinc Granules	0.05 mA	99%	82.6 +/− 4.0%

layer, or a combination of both, limit the time to passivation. For a diffusion dominated process, the relationship between current and time to passivate is generally of the form:

$$(i - i_e)\, {t_{pass}}^{1/2} = k \quad [11]$$

where k are i_e are system constants that depend on system parameters such as geometry, particle surface area, diffusion parameters and discharge current. Therefore, the utilization loss related to passivation can be represented by:

$$Utilization_{passivation} = \frac{Q_{pass}}{Q_{total}} = \frac{i_{disc} * t_{pass}}{Q_{total}}$$
$$= i_{disc} * k^2/[Q_{total} * (i_{disc} - i_e)^2] \quad [12]$$

Where the charge passed until the system passivates, Q_{pass}, is given by the product of the discharge rate and time until passivation: $Q_{pass} = i_{disc} * t_{pass}$. In this passivation-controlled case, it is t_{pass} that determines utilization, whereas in the corrosion case, the parasitic current acts concurrently with discharge to reduce utilization. In general terms, this implies that the greater the particle surface area, the longer the time will be until passivation,[16] as the porous type I ZnO passivation layer that forms over the zinc surface will have a reduced thickness for higher surface area zinc, reducing diffusion limitations. Figure 5 shows this passivation effect (red dot-dash line). At low currents, loss in utilization from passivation effects is negligible. As current increases, passivation effects become more significant, and ultimately are the main factor limiting total utilization. It should be noted that this model description only applies to diffusion related passivation, and does not capture the onset of solid-state formation of type II ZnO,

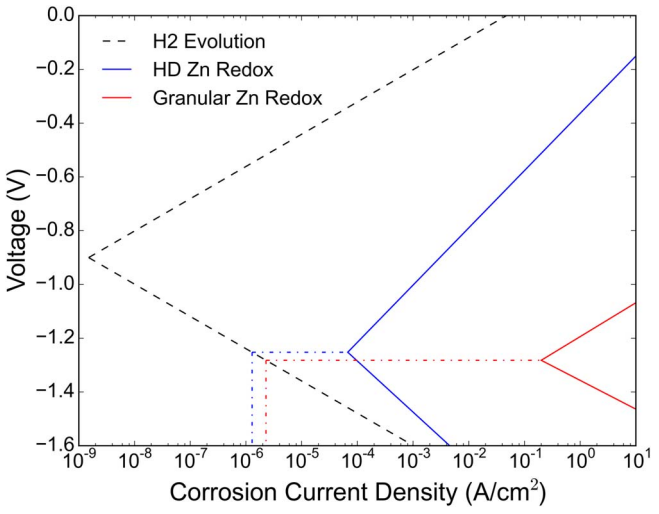

Figure 6. Evans diagram of corrosion on zinc. The dashed black line represents the hydrogen evolution half reaction, and the solid blue and red lines represent the zinc dissolution half-reactions of HD and granular zinc, respectively. This reaction is kinetically-limited by hydrogen evolution. The total corrosion current is given by the corrosion current density acting over the reaction surface area. Despite the corrosion current density being slightly lower for HD Zn than granular zinc, the overall corrosion rate is higher on account of the higher surface area of HD Zn.

which will affect utilization at the highest currents and near the end of useful discharge capacity.

The result of combined utilization under both passivation and corrosion effects (solid black line) can also be seen in Fig. 5 (excluding current collector contact effects). Combined, these two mechanisms predominantly describe the behavior seen in Fig. 4, including the crossover effect between low and high current regions. At low currents, in the corrosion dominated regime, as corrosion is proportional to time and area, we find that the zinc granules and dust perform better. As particle surface area increases, the corrosion dominated segment of the graph shifts to the right, and this is clearly seen in the case of the HD Zn. Moving to higher currents, passivation becomes the dominant regime, and utilization then decreases with increasing discharge rate. While there is not an explicit dependence on particle surface area in the passivation dominated region, it should be noted that k is heavily dependent on the system parameters, and current density is one determining factor on k.

A third mechanism which will affect utilization at both low and high current regimes is loss of zinc contact with the current collector, electrically isolating particles.[23] This could happen in two ways: the formation of a passivating layer at the zinc/current collector interface, or local dissolution of zinc from the interface creating a physical gap between the zinc and current collector. We would expect that both of these mechanisms may affect the HD Zn to a greater degree than the granular zinc.

Given the fine featured, branched structure of the HD Zn (Figs. 2 and 3), several morphological differences will exist during dissolution. Re-orientation of the branched particles with respect to each other in HD Zn will be more difficult than is the case for granular zinc, where particles are free to reorient to new positions due to a smaller number of contact points with surrounding particles. We would expect that a granular zinc particle can settle onto the current collector surface as dissolution occurs, where as a hyperdendritic zinc branch would have many contact points with surrounding HD Zn particles, and would not necessarily be free to resettle onto the current collector surface during dissolution. Thus, during discharge we may expect that the contact area of zinc with the surface may decrease more rapidly for HD Zn, potentially isolating zinc material from discharge and lowering utilization.

In addition, given the increased tortuosity of electrolyte in reaching the zinc/current collector interface in the case of the HD Zn, a passivation layer would also be more likely to build in those locations. This would be related to depletion of OH- ions and saturation of zincate causing a passivation layer to build at the particle/current collector interface. These effects together would likely be a cause of reduced utilization at low currents compared with the estimated utilization under a corrosion only effect. Figure 7 illustrates this concept.

Figure 8 shows electrochemical impedance spectroscopy (EIS) during discharge on both HD and granular zinc particles at a rate of 0.2 A/g. We can extract the charge transfer resistance (R_{ct}) from the EIS data, using an electrochemical cell equivalent model in the kinetic control region (no diffusion). The model utilized was an ohmic resistance in series with a charge transfer resistance and double layer capacitance (represented as a constant phase element) in parallel. For both particle types, we observe that R_{ct} increases during discharge. Plotting R_{ct} versus state of charge (SOC), we can see that R_{ct} increases more rapidly for the HD Zn than for the granular zinc, supporting the argument that isolation affects HD Zn more than granular zinc. At the

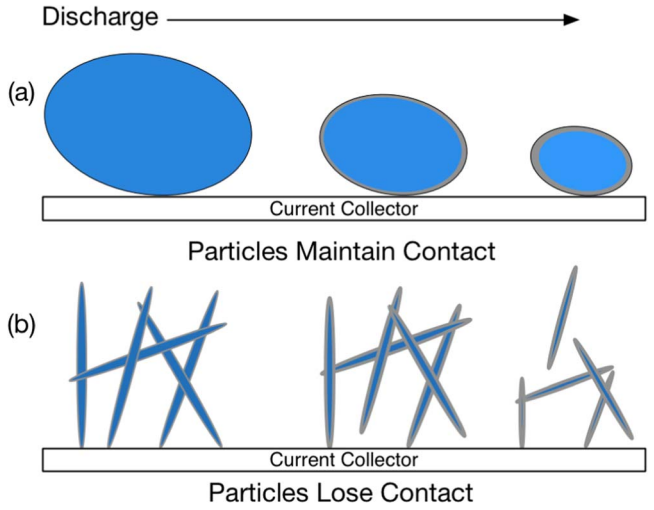

Figure 7. Evolution of particle contact and isolation during discharge. The granular and dust morphologies are more likely to maintain good contact with the current collector surface during discharge. The HD Zn is more likely to lose current collector contact during discharge.

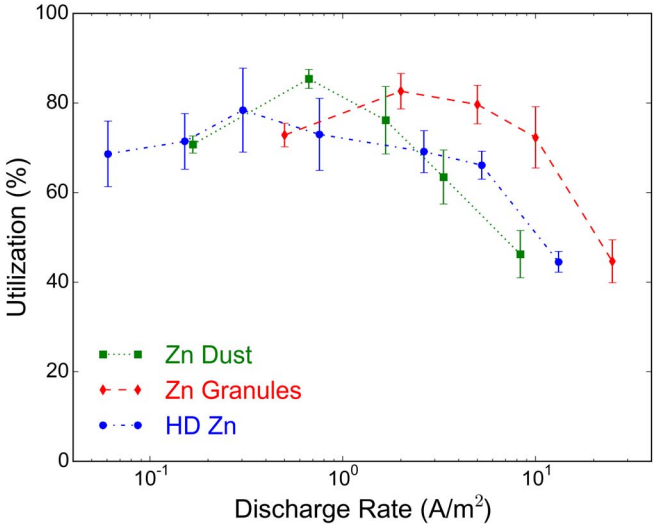

Figure 9. Comparison of surface area normalized current (current density), showing the impact on utilization. On a particle surface area basis, zinc granules perform the best, however this does not take into account bulk diffusion towards/away from the projected electrode surface area, or tortuosity effects present for HD Zn or zinc dust.

end of charge, we see a dramatic increase in R_{ct} for HD Zn, which is consistent with complete isolation of zinc from the current collector surface due either to loss of contact or passivation. Upon visual inspection of the samples post-discharge, for HD Zn we observed active material floating away from the current collector for HD Zn but not granular zinc, which is qualitatively consistent with the EIS data.

Despite this effect also being apparent in high current regimes, the HD Zn still performs significantly better than the granular zinc and zinc dust. Considering the high current passivation controlled region, at rates of 1.0 A/g and above we clearly see that HD Zn outperforms the other morphologies in terms of utilization. While there is some reduction in utilization as current increases, the relative performance gap between HD Zn and the other zinc forms improves significantly as current is increased. At a rate of 2.5 A/g, the utilization of HD Zn is 50% higher than that of the other two Zn morphologies. At 10 A/g and higher, the utilization is effectively zero for the granules and dust, whereas HD Zn still performs well, showing utilization of 66 and 45% at 10 and 25 A/g respectively. At high rates, the excellent performance of the HD Zn is displayed.

In this high current regime, parasitic corrosion mechanisms only form a small proportion of the total utilization loss, as illustrated in the model. Now a blocking passivation layer becomes the primary mechanism limiting zinc utilization. In the case of all of the zinc types, a more rapid discharge leads to a decrease in utilization. One factor leading to an increase in the rate of passivation is an increase in current density (mA/cm^2), which decreases the k parameter in 12.[16] Therefore, as expected, the HD Zn performs significantly better at higher absolute currents, given its order of magnitude higher surface area, and correspondingly lower surface-area-normalized current density.

To further understand the the effects of surface area, we ran a series of additional experiments to provide data to normalize the current on a particle surface area basis (rather than projected electrode area basis). This gave an effective current density based on the surface area of the particles. Experiments were run at currents of 10 and 25 A/g on Zn granules and HD Zn. At these high currents, the Zn granules passivated almost immediately, giving a utilization of near zero. However discharge of the HD Zn was still possible, based on the high surface area characteristic of this morphology.

Figure 9 shows the utilization efficiency versus current density normalized for particle surface area. This gives a surface current density comparison of the three particles types, rather than a comparison of absolute current for a given mass of zinc as previously. It should be noted that particle surface current density is not the only factor that impacts passivation and the ultimate utilization, however it allows for some comparison and determination of the relative importance of surface area to the overall performance of the HD Zn. On a current density basis there is a difference visible between the two morphologies. The Zn dust and HD Zn display a similar levels of utilization with current density normalized by surface area. On a current density

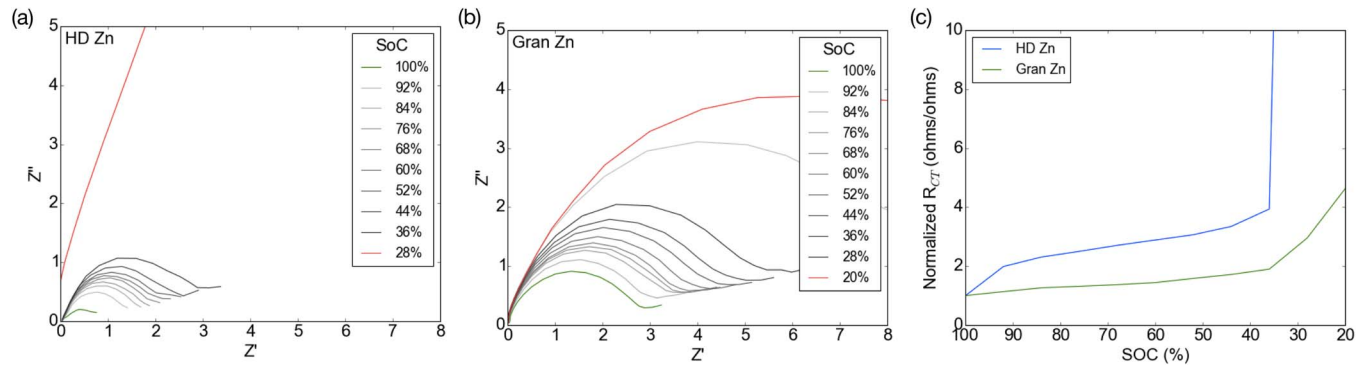

Figure 8. Progression of the AC impedance (EIS) response of (a) HD Zn and (b) granular zinc during discharge. Plot (c) shows how R_{ct} evolves versus state of charge (SOC); R_{ct} is normalized by the initial R_{ct}. The increase in normalized R_{ct} during discharge is more dramatic for HD Zn compared with granular Zn.

basis, however, the zinc granules perform best, with the same general trend shifted to higher current densities. If utilization were only a particle surface area effect, we would expect to see all lines collapse onto a single line, however it is clear other mechanisms come into play.

At any given current density, the absolute current applied to the cell is an order of magnitude larger for the HD Zn compared with the other morphologies. For example, at a given current density, the HD Zn electrode requires an order of magnitude greater diffusion of OH^- ions to the surface, and $Zn(OH)_4^{2-}$ ions away from the surface. Therefore the effects of zincate supersaturation will be felt more strongly on the HD Zn, leading to faster passivation. Tortuosity effects will also be important for the Zn dust and HD Zn types, as there is no straight path between the surface of the particles and the current collector given that the particles do not form a monolayer on the current collector, unlike granular zinc. Therefore zincate ions will take a longer time to diffuse through the porous electrode (and OH^- to the particles), causing a local zincate buildup above the saturation limit, again leading to earlier passivation. Still, on an absolute current basis, the superior performance of HD Zn is demonstrated.

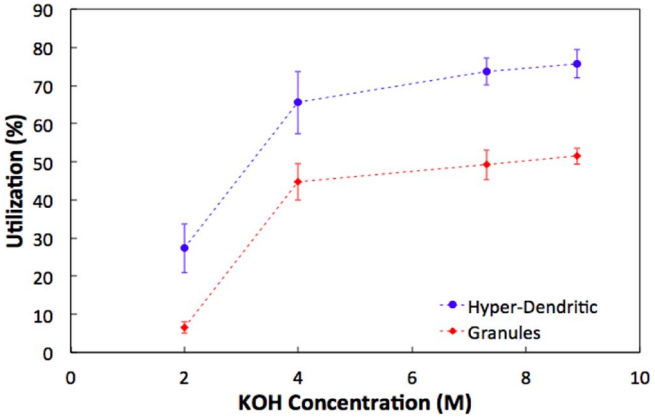

Figure 10. Effect of KOH concentration on % utilization of HD-Zn and granules, as measured from galvanostatic discharge at 2.5 A/g in solutions with a range of KOH concentrations.

Studying the effect of electrolyte additives.—Given the clear benefits of HD Zn in providing a high rate discharge capability, and reducing the negative impacts of formation of a blocking passivation layer, a range of additives were tested with the HD Zn to confirm whether high-rate discharge performance could be further improved.

First, the impact of electrolyte concentration was studied on this system. Given the similar performance of granules and dust, only granules and HD Zn were used for this investigation. Zn granules and HD Zn were discharged at 2.5 A/g in aqueous potassium hydroxide (KOH) electrolytes with KOH concentrations ranging from 2–8.9 M. The % utilization results are shown in Figure 10. For both particle types utilization increases with concentration, with the largest rate of utilization increase between 2 and 4 M KOH. At all KOH concentrations, HD Zn has a significantly higher utilization than Zn granules. This trend in utilization with increasing electrolyte molarity is expected, as it is known that the solubility of ZnO in aqueous KOH solutions is a non-linear function of the KOH concentration, and that passivation during anodic dissolution is impacted by the local saturation of zincate at the surface of Zn particles.[1]

Further study was completed on a range of additives to explore their benefits on utilization at fixed electrolyte KOH concentration. The study focused on 8.9 M KOH electrolytes, and four additives were considered: potassium citrate (K-citrate), potassium chloride (KCl), sodium dodecylbenzenesulfonate (SDBS), and zinc oxide (ZnO). Figure 11a shows the percentage gain in utilization for each of the additives for both granular and HD Zn over their baseline utilizations without additives. Both KCl and K-citrate provide significant utilization gains for the HD Zn, in the 7–10% range, however only a marginal gain was shown with addition of SDBS. The granular Zn shows excellent improvement in utilization with the KCl and K-citrate additives, however it is starting from a lower base utilization. Unlike the HD Zn, there is also a significant improvement in granule utilization by the addition of SDBS.

As discussed previously, the K-citrate and KCl additives are understood to improve performance through complexing with the Zn^{2+} ion, and increasing its solubility compared with that of the zincate ion alone. In the presence of SDBS, a surfactant, the utilization efficiency of dendritic Zn does not appear to significantly change, however the utilization efficiency of Zn granules is improved. Evidence in the literature suggests that in the presence of SDBS, the passivation layer that forms is more porous than in the absence of the surfactant,[21] meaning that even as a ZnO film forms during discharge, the pores in the passivation layer result in electrolyte maintaining access to the Zn surface. Therefore, dissolution will continue, at least until OH^- transport in the pores cannot keep up with the depletion rate.[16]

For a simple surface morphology, like that of the granular zinc, these pores maintain access for the electrolyte to the zinc. For a more complex surface morphology, the benefits of a porous passivation layer may be less pronounced, as the pathways to access the zinc surface are already tortuous, and passivation layers may overlap. In addition, for the HD Zn, the passivation layer is less thick than the

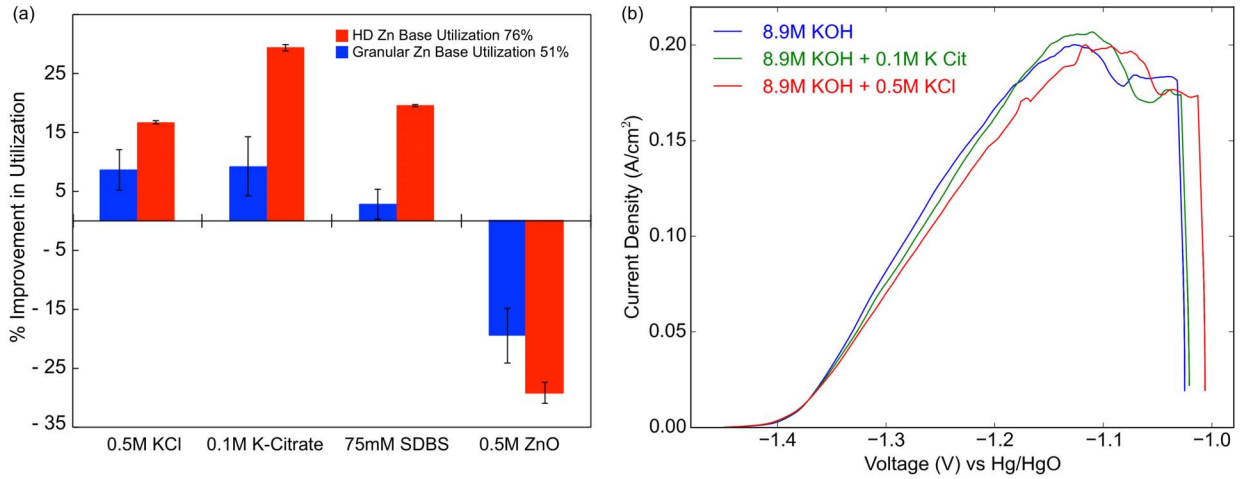

Figure 11. Comparison of the effect of electrolyte additives (a) on % utilization of HD-Zn and granules, measured at a discharge current of 2.5 A/g (~3C discharge rate). (b) shows the delay in the onset of passivation for the electrolytes with K-cit and KCl additives using linear sweep voltammetry on planar zinc.

granular Zn, which already results in a higher utilization. Figure 3 shows the significantly larger surface area of the HD Zn during discharge, minimizing the benefit of increasing porosity in the already thin passivation layer.

To further understand the benefits of the additives on zinc utilization, as shown in Figure 11b, linear sweep voltammetry (LSV) was run on the base electrolyte and the two most beneficial additives for the HD Zn: K-Citrate and KCl. The onset of passivation in the electrolyte containing KCl is increased by 20mV compared with the baseline 8.9 M KOH electrolyte, which points to delayed passivation and thus increased utilization. The passivation potential in the K-Citrate electrolyte is similar to that of the baseline, however it is noted that the peak current is higher, suggesting a less blocking type I zinc oxide layer forming on the surface of the zinc.

As expected, addition of ZnO significantly reduced the utilization of both zinc morphologies at higher currents. The addition of ZnO increases the zincate concentration. As Zn discharges, the solution locally saturates more quickly, and a blocking passivation layer forms more readily on the Zn surface, significantly reducing the Zn utilization.[16] It should be noted that at very low discharge rates, where corrosion effects dominate, the addition of ZnO is beneficial due to the suppression of the hydrogen evolution reaction.[1]

Conclusions

We explored the performance of several zinc morphologies in a freestanding, flooded system with no binders or conductive additives. The utilization of each particle type was studied for a range of different electrolyte concentrations and additives at varying discharge rates.

Even in non-optimized electrolyte, hyper-dendritic zinc performed very well at high discharge rates (>2.5 A/g), showing zinc utilization 50% higher than other zinc morphologies. At rates of 10 A/g and higher, the zinc dust and zinc granules showed no discharge capacity, effectively passivating instantaneously. However, the hyper-dendritic zinc continued to perform well, showing utilization above 65% at these high rates.

The significantly higher surface area and complex structure of the hyper-dendritic zinc, typically within the range of 1.9–3.6 m^2/g, is beneficial for reducing the passivation effects seen at high currents. SEM images show that the hyper-dendritic zinc morphology retains its dendritic nature during discharge (Figure 3). This has the effect of maintaining a high surface area during discharge. In addition, this provides a high surface area substrate for re-plating of zinc during charge, further confirming its cyclability as previously investigated.[12]

At low currents, while corrosion effects on the HD Zn result in a lower utilization, there appears to be an additional contribution to utilization loss through active material losing contact with the current collector and becoming isolated. Therefore, even better performance of hyperdendritic zinc may be possible in non-freestanding configurations.

Further utilization efficiency gains are possible with optimization of the electrolyte and additives. High concentration KOH electrolytes lead to significant gains in utilization. The addition of either potassium citrate or potassium chloride to the electrolyte improves the utilization of HD Zn by 9% for both additives, and the performance of the zinc granules by 17 and 30% respectively. Both of these additives are believed to act through complexation with the zinc ion, which subsequently increase the complex solubility, hindering passivating layers from building on the zinc surface. These have been demonstrated to give excellent performance gains.

SDBS was found to marginally increase the performance of the HD zinc, however significantly improved the performance of zinc granules. This effect acts through increasing the porosity and decreasing the density of passivation layers formed, so that active zinc dissolution can still take place.

Overall, and critically, at discharge currents >2.5 A/g, hyperdendritic zinc significantly outperforms zinc granules and zinc dust. This suggests both primary and secondary battery systems using a zinc anode could benefit significantly by using HD Zn, allowing much higher discharge rates, improved utilization and efficiency in systems where the zinc anode has typically been a limiting element.

Acknowledgments

This work was supported in part by NSF CBET 1318163, the Andlinger Center for Energy and the Environment and Princeton Environmental Institute Grand Challenges Fund, the Princeton Project X Fund, and the Princeton E-ffiliates Fund.

References

1. X. G. Zhang, *Corrosion and Electrochemistry of Zinc*, Springer US, (1996).
2. A. P. Karpinski, B. Makovetski, S. J. Russell, J. R. Serenyi, and D. C. Williams, *J. Power Sources*, **80**, 53 (1999).
3. K. Bass, P. J. Mitchell, G. D. Wilcox, and J. Smith, *J. Power Sources*, **35**, 333 (1991).
4. D. Linden and T. B. Reddy, *Handbook of Batteries*, 3rd Edition, McGraw-Hill, (2002).
5. J. F. Parker, C. N. Chervin, E. S. Nelson, D. R. Rolison, and J. W. Long, *Energy Environ. Sci.*, **7**, 1117 (2014).
6. T. Reddy, *Linden's Handbook of Batteries*, 4th Edition, 4 edition., McGraw-Hill Education, (2010).
7. B. Dunn, H. Kamath, and J.-M. Tarascon, *Science*, **334**, 928 (2011).
8. Y. Ito et al., *J. Power Sources*, **196**, 2340 (2011).
9. S. I. Smedley and X. G. Zhang, *J. Power Sources*, **165**, 897 (2007).
10. J. F. Cooper, US Pat. (1995) https://www.google.com/patents/US5434020.
11. L. Zhang et al., *J. Power Sources*, **179**, 381 (2008).
12. M. Chamoun et al., *NPG Asia Materials*, **7**, e178 (2015).
13. M. Hilder, O. Winther-Jensen, B. Winther-Jensen, and D. R. MacFarlane, *Phys. Chem. Chem. Phys.*, **14**, 14034 (2012).
14. M. C. H. Mc Kubre and D. D. Macdonald, http://jes.ecsdl.org/content/128/3/524.full.pdf.
15. R. W. Powers and M. W. Breiter, *J. Electrochem. Soc.*, **116**, 719 (1969).
16. M. Liu, G. M. Cook, and N. P. Yao, *J. Electrochem. Soc.*, **128**, 1663 (1981).
17. A. J. Salkind, F. McLarnon, and F. Bagotzki, *Proceedings of the Symposium on Rechargeable Zinc Batteries: Commemorating the 100th Birthday of A. N. Frumkin*, Electrochemical Society, (1996).
18. J. W. Gallaway et al., *J. Electrochem. Soc.*, **161**, A275 (2014).
19. R. Renuka, S. Ramamurthy, and K. Muralidharan, *J. Power Sources*, **76**, 197 (1998).
20. S. Peulon and D. Lincot, *J. Electrochem. Soc.*, **145**, 864 (1998).
21. H. Yang, Y. Cao, X. Ai, and L. Xiao, *J. Power Sources*, **128**, 97 (2004).
22. A. M. Gaikwad, D. A. Steingart, T. N. Ng, D. E. Schwartz, and G. L. Whiting, *Appl. Phys. Lett.*, **102**, 233302 (2013).
23. Y. Shen and K. Kordesch, *J. Power Sources*, **87**, 162 (2000).
24. A. Stani, W. Taucher-Mautner, K. Kordesch, and J. Daniel-Ivad, *J. Power Sources*, **153**, 405 (2006).
25. Y. Sharma, A. Haynes, L. Binder, and K. Kordesch, *J. Power Sources*, **27**, 145 (1989).